Gate Drive Power Supply with Low Insulation Voltage Transformer for in-vehicle Marx Circuit

Keisuke Kusaka
Dept. of Electrical Electronics, and Information Engineering
Nagaoka University of Technology
Nagaoka, Niigata, Japan
kusaka@vos.nagaokaut.ac.jp

Yosuke Ouchi
Dept. of Electrical Electronics, and Information Engineering
Nagaoka University of Technology
Nagaoka, Niigata, Japan
s195026@stn.nagaokaut.ac.jp

Jun-ichi Itoh
Dept. of Electrical Electronics, and Information Engineering
Nagaoka University of Technology
Nagaoka, Niigata, Japan
itoh@vos.nagaokaut.ac.jp

***Abstract*—This paper proposes a gate drive circuit with a low-insulation voltage transformer for an in-vehicle Marx circuit. The Marx circuit will be used for NOx gas decomposition for diesel vehicles as a part of an ozonizer. In order to make the Marx circuit on board, it is necessary to reduce the size and cost of the circuit, including the gate drive circuits. One of the bottlenecks for lowering the cost and size of the gate drive circuit is the insulation transformers on the gate drive circuits because the potential of each switch of the Marx circuit dynamically changes from zero to the output voltage of the Marx circuit. This paper proposes and demonstrates the gate drive circuit, which receives the drive power for the MOSFET on the *n*-th stage from (*n* – 1)-th stage through a low-voltage transformer. Due to the configuration, the required insulation voltage of the transformer is equal to the input voltage. In this paper, the design procedure of the transformer with an approximated current is described. The proposed gate drive circuit is developed and implemented to the 4-kV Marx circuit.**

Keywords—Gate drive, Marx circuit, Insulation

I. INTRODUCTION

In recent years, reducing nitrogen oxide (NOx) gas in exhaust gas from diesel vehicles has been a critical issue to curb global warming. Thus, the regulation of NOx gas in exhaust gas has been tightened globally. A lean NOx trap catalyst (LNT catalyst) has been used [1–2]. The LNT catalyst adsorbs NOx gas; however, the adsorb efficiency is degraded when the exhaust gas temperature is low. In order to improve the adsorb efficiency, in-vehicle use of an ozonizer is being considered [3–4]. The ozonizer produces ozone and adds to the exhaust gas to reform NO into NO_2. The NO2 is absorbed by the LNT catalyst with high efficiency.

The ozonizer needs a pulse power supply, such as the solid-stage Marx circuit [5–7]. Especially, silicon carbide (SiC) MOSFETs have been used in the Marx circuit with the progress of SiC semiconductor technology in recent years instead of conventional silicon (Si) MOSFETs [8–10]. SiC MOSFETs provide a fast switching with high-drain-source voltage, such as 1.2 or 1.7 kV [11]. The fast switching improves the production performance of the ozone.

There is a strong demand for price and volume reduction for onboard circuits [12]. However, the Marx circuit with MOSFETs has a bottleneck on the gate drive circuits for reducing the volume and cost. The *n*-stage Marx circuit needs 2*n* switches and gate drive circuits. Each gate drive circuits require an isolated power supply with high-withstand voltage because the potential of MOSFETs is dynamically changed due to the operation of the Marx circuit. The typical withstand voltage of isolated power supplies on the market for gate drive is less than 5 kV. Thus, a custom-built isolated DC/DC converter is required.

In order to overcome the problem mentioned above, the gate drive power supply combined with the Marx circuit is proposed. In the proposed gate drive power supply, the drive power for *n*-stage MOSFET is supplied from the (*n* - 1)-th stage through the low-voltage transformer, which is inserted into the charging path of the Marx circuit [13–14]. It contributes to reducing the cost and size of the transformer. Besides, the inserted transformers are a help to reduce the peak of the charging current of the Marx circuit.

II. PROPOSED GATE DRIVE POWER SUPPLY

A. Marx Circuit

Figure 1 shows the Marx circuit with the proposed gate drive power supply [12]. The Marx circuit outputs high-voltage by changing the connection of the Marx capacitor C_n. When the switches S_{cn} turn on, the Marx capacitors are connected in parallel. The Marx capacitors are charged through the diodes D_n. Each Marx capacitor is charged to the input voltage by ignoring the forward voltage drop of the diodes. In contrast, the Marx capacitors are connected in series when the switches S_{Dn} turn on. Because the Marx capacitors are charged to the input voltage during the previous charging operation, the output voltage is *n* times of the input voltage V_{in} ideally.

Each stage of the Marx circuit has two MOSFETs and a diode. The gate drive circuit is connected to each MOSFET to drive the device. The gate drive circuit for the *n*-stage are driven with the power supplied from the (*n* - 1) stage through the additional transformers Tr_n. The detail of the power supply is explained in the next section.

B. Operation Principle of Gate Drive Power Supply

Figure 2 shows the proposed gate drive power supply. The thick wire is the main circuit of the Marx circuit. The gate drive power for S_{Cn} is supplied from the transformer $Tr_{(n-1)}$. The primary side of the transformer is connected on the charging path on the Marx circuit. During the charging path, the charging current of the Marx capacitor flows on the primary winding. On the secondary side of the transformer,

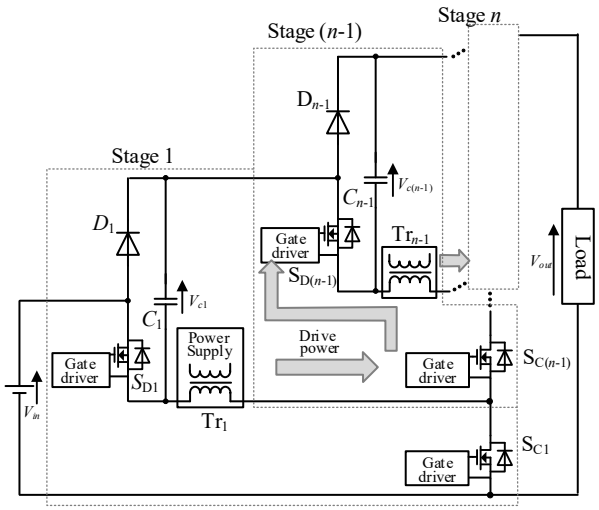

Fig. 1. Marx circuit and proposed gate drive supply.

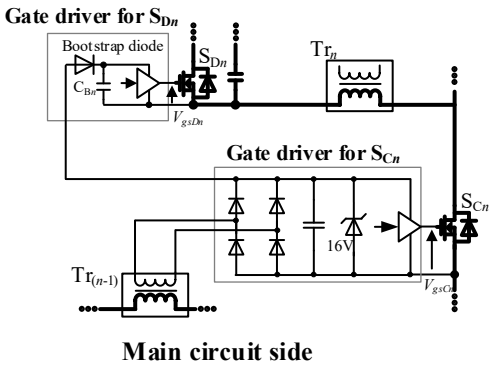

Fig. 2. Proposed Gate drive supply.

the voltage is induced. The induced voltage is supplied to the gate drive circuit for S_{Cn} through the full-bridge rectifier. Note that the Zener diode is connected to clamp the gate drive voltage at 16 V. The switch S_{Cn} turns on or off with the supplied power. For the gate drive circuit of S_{Dn}, the bootstrap circuit is used [15–17]. The DC line of the gate drive circuit for S_{Cn} is connected to the gate drive circuit for S_{Dn} via the bootstrap diode. When the switch S_{Cn} turns on, the current charges the bootstrap capacitor C_{Bn} through the bootstrap diode, transformer Tr_n, and S_{cn}. The reverse blocking voltage of the bootstrap diodes must be higher than the input voltage of the Marx circuit.

The required insulation voltage of the proposed topology is as same as the input voltage. Thus the volume of the isolation transformer is reduced.

III. Design of Isolation Transformer

In this chapter, the design method of the insulation transformer is discussed. Table I shows the requirements for the insulation transformers for the conventional and the proposed gate drive supply. The conventional gate drive supply needs the transformer to supply the power from an auxiliary power supply to the gate driver. The primary voltage is arbitrary because it depends on the voltage of the auxiliary power supply. The secondary voltage should be equal to the

TABLE I. Requirements for Isolation Transformer.

	Conventional	*Proposed*
Maximum primary voltage	Arbitrary	$V_{in} - V_{cj(0)}$
Secondary voltage	V_{gs}	V_{gs}
Insulation voltage	jV_{in}	V_{in}

[a.] j denotes the jth stage in the Marx circuit with n stages.

gate-source voltage V_{DS}. In the conventional system, the transformer must ensure the high-voltage insulation jV_{in} because the auxiliary power supply is grounded. Note that, j notes the jth stage in the n stages Marx circuit.

In contrast, the difference between the input voltage V_{in} and the Marx capacitor voltage $V_{cj(0)}$ is applied on the primary side of the proposed topology at the start of the charging operation. Note that the Marx capacitor voltage is discharged and maintained at a lower voltage than input voltage in the previous discharging operation. The required insulation voltage of the transformer is as same as the input voltage because the voltage difference between the primary and secondary sides is the Marx capacitor voltage at the maximum.

A. Modeling of Secondary Current

In this section, the current on the transformer is analyzed to design the transformer.

Figure 3 shows the simplified equivalent circuit at the charging operation. The charging current must be modeled for the transformer design because the supplied voltage on the secondary side depends on the primary current. Moreover, the added primary inductance also affects the charging operation. First, the charging current i_1 and i_2 are calculated. From Fig. 3, equations (1) is developed assuming the DC capacitors of the rectifier is large enough to maintain the voltage V_D, where V_{in} is the input voltage of the Marx circuit, L_1 is the primary self-inductance, L_2 is the secondary self-inductance, L_{1leak} and L_{2leak} are the leakage inductance of the transformer, L_M is the mutual inductance, R is the parasitic resistance of the Marx capacitor and switches, and C_n is the Marx capacitor.

$$\begin{cases} V_{in} - V_{Cn(0)} = L_1 \dfrac{di_1}{dt} + L_M \dfrac{d(i_1 - i_2)}{dt} + \dfrac{1}{C_n}\int i_1 dt + Ri_1 \\ V_D = L_M \dfrac{d(i_2 - i_1)}{dt} + L_2 \dfrac{di_2}{dt} \\ L_M = k\sqrt{L_1 L_2} \end{cases} \quad (1)$$

The Marx capacitor voltage is charged because the Marx capacitor was discharged to $V_{Cn(0)}$ due to the previous discharging operation. At $t = 0$, the switch turns on. Then the charging operation starts.

The secondary current $i_{2(t)}$ is developed from (1).

$$i_{2(t)} = \frac{k\left(V_{in} - kV_D - V_{Cn(0)}\right)}{\sqrt{\frac{\beta}{C_n} - \left(\frac{R}{2}\right)^2}} e^{-\frac{R}{2\beta}t} \sin\sqrt{\frac{1}{\beta C_n} - \left(\frac{R}{2\beta}\right)^2}\, t - \frac{kV_D}{L_{1leak} + L_M} t \quad (2)$$

where $\beta = (L_{1leak} + L_M - kL_M)$.

B. Design of Inductance for Transformer

From (2), the inductance to supply the required gate drive power is calculated. In order to analytically solve the equation, (2) is approximated, as

$$i_{2(t)} \approx \frac{k\left(V_{in} - kV_D - V_{Cn(0)}\right)}{\sqrt{\frac{\beta}{C_n} - \left(\frac{R}{2}\right)^2}} e^{-\frac{R}{2\beta}t} \sin\sqrt{\frac{1}{\beta C_n}}\, t \quad (3)$$

with the assumption that the voltage drop on the on-resistance of the MOSFETs is zero, and the second term in (2) can be ignored because the first term is dominant in several microseconds during the transient response.

Figure 3 shows the calculation of the secondary current $i_{2(t)}$ expressed as (2) and (3). By the approximation, the time to reach the maximum current t_2 and the time to reach the zero t_1 is easily calculated with low error.

$$t_1 \approx \sqrt{(L_{1leak} + L_M - kL_M)C_n}\,\pi \quad (4)$$

$$t_2 \approx \frac{\sqrt{(L_{1leak} + L_M - kL_M)C_n}\,\pi}{2} \quad (5)$$

$$i_{\max} \approx \frac{k\left(V_{in} - kV_D - V_{Cn(0)}\right)}{\sqrt{\frac{L_{1leak} + L_M - kL_M}{C_n} - \left(\frac{R}{2}\right)^2}} \quad (6)$$

Using the approximated time t_1 and t_2 and peak current, the supplied power highlighted in Fig. 3 is calculated as

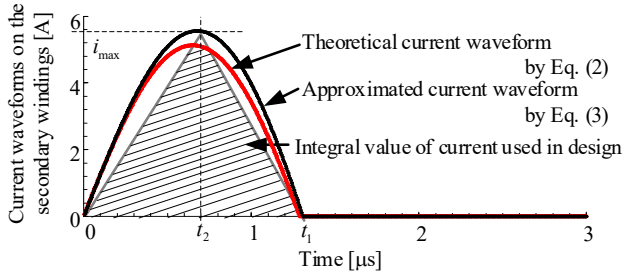

Fig. 3. Marx circuit with proposed gate drive power supply.

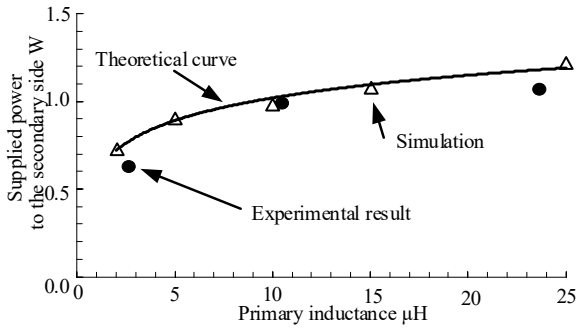

Fig. 4. Self-inductance and supplied power.

$$P_{out} = f_{sw} V_{out} \frac{k\left(V_{in} - kV_D - V_{Cn(0)}\right)}{\sqrt{\frac{L_{1leak} + L_M - kL_M}{C_n} - \left(\frac{R}{2}\right)^2}} \sqrt{(L_{1leak} + L_M - kL_M)C_n}\,\pi \quad (7),$$

where P_{out} is the output power of the gate drive power supply.

Thus, the required self-inductance for the transformer is expressed as

$$L_1 = \frac{C_n R P_{GD}^{\ 2}}{(1-k^2)\left[4P_{GD}^2 - C_n\left\{f_{sw} V_D \pi k\left(V_{in} - kV_D - V_{Cn(0)}\right)\right\}^2\right]} \quad (8),$$

where P_{GD} is the power consumption of two gate drive circuits.

C. Drive power and inductance

Figure 4 shows the relation between the supplied drive power and the self-inductance of the transformer. The solid line is the theoretical curve calculated from (2) by a numerical analysis. The triangles represent the calculated power by the circuit simulation. The circle represents the experimental results. The experimental results show good agreement with the simulation and the theoretical curve. It implies that the effect of the approximation on (2) is small enough to be ignored.

IV. Experimental Verification

The Marx circuit with the proposed gate drive power supply is demonstrated in this chapter. Table II shows the specifications of the prototype. The input voltage is derated from 1 kV to 600 V due to the limitation of the power supply in the Lab. Moreover, the number of the stage is seven.

Figure 5 shows the prototype of the Marx circuit with the proposed power supply. Fig. 4 (a) is the Marx circuit and the capacitor load. Fig. 4 (b) is the isolation transformer for the gate drive power supply. The primary and the secondary windings are placed with a gap of 10 mm for insulation. The isolation transformer for the Marx circuit can be downsized because the required isolation voltage is as same as the input voltage. Note that the capacitor load is used as the load instead of an ozonizer.

Figure 6 shows the output voltage of the Marx circuit. The output voltage of 4 kV is obtained. Fig. 5 (a) and (b) shows the expanded waveforms focusing on the positive edge and the

TABLE II. SPECIFICATIONS.

Parameters	Symbols	Value
Input voltage	V_{in}	600 V
GDU voltage	V_D	16 V
Marx capacitor	C_n	0.22 μF
Switching frequency	f_{out}	10 kHz
on-resistance of MOSFETs	R	0.5 Ω
Coupling coefficient	k	0.95
Primary leakage inductance	L_{leak1}	$(1\text{-}k)L_1$
Secondary leakage inductance	L_{leak2}	$(1\text{-}k)L_1$
Primary inductor	L_1	10.5 μH
Magnetic core for trans.		PC44 (TDK)
Number of stage	n	7
Discharging time		6 μs
MOSFETs		C3M0065100J (CREE)
Load	C_{out}	500 pF

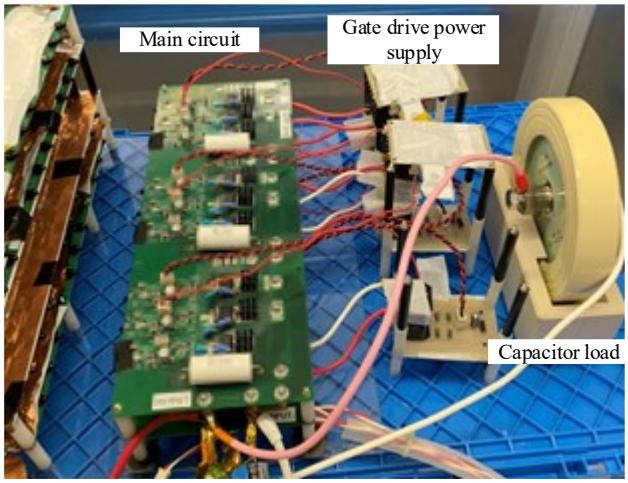

(a) Marx circuit and capacitor load.

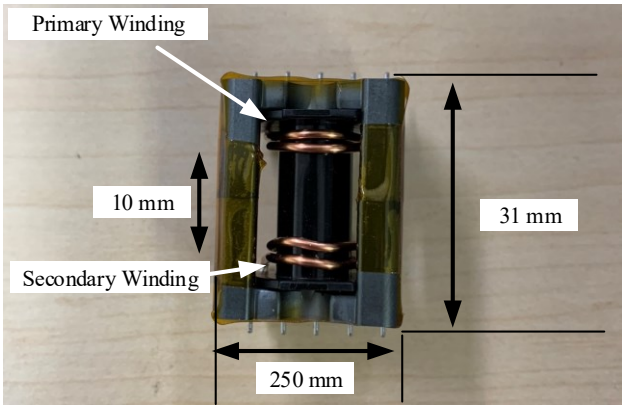

(b) Insulation transformer for gate drive power supply

Fig. 7. Prototype of the Marx circuit with proposed gate drive power supply.

negative edge, respectively. The rise time and fall time of the output voltage is less than 100 ns.

Figure 7 shows the switching waveforms from the discharging operation and the charging operation. At the charging operation, the secondary current flows on the transformer and the diode bridge rectifier. The gate drive

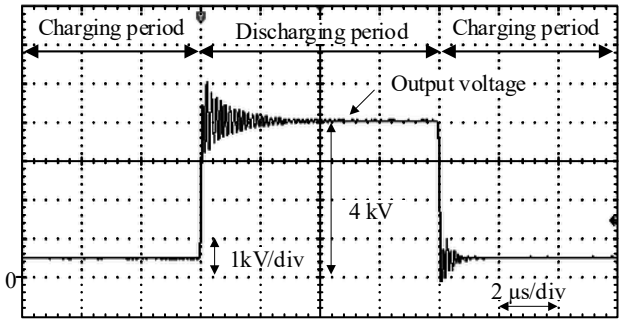

(a) Charging and Discharging opoerations.

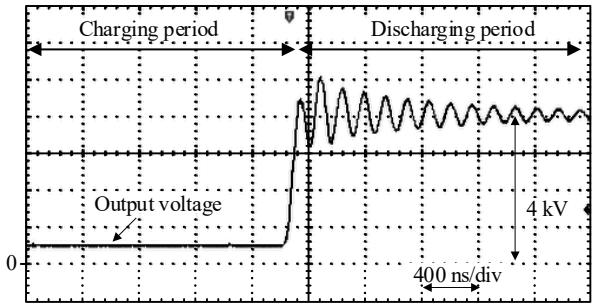

(b) Positive edge.

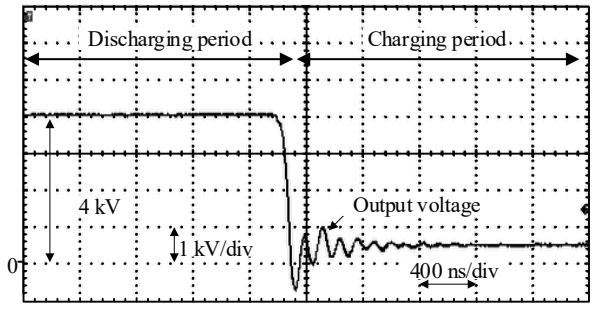

(c) Negative edge.

Fig. 5. Output voltage of the Marx circuit.

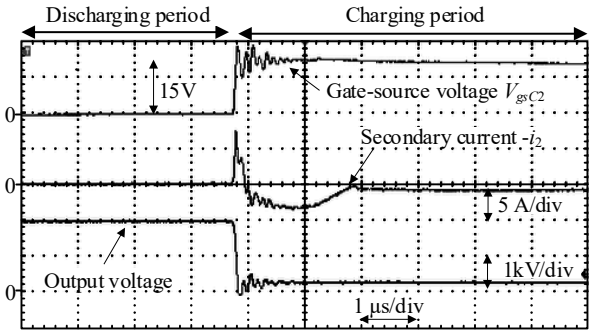

Fig. 6. Power supply to the gate drive circuit during charging operation.

power for MOSFETs is supplied through the proposed isolation system with a low-voltage transformer.

V. Conclusion

A gate drive circuit with a low-voltage transformer for an in-vehicle Marx circuit is proposed in this paper. The downsizing and cost reduction are required to mount the Marx circuit on board. One of the bottlenecks of the cost reduction is the gate drive power supply because high-voltage isolation is required due to the operation of the Marx circuit. In order to reduce the cost and size of the isolation transformer, a new gate drive power supply is proposed. The gate drive power for MOSFETs on the n-th stage is supplied from $(n-1)$-th stage via the low-voltage transformer. The proposed topology is demonstrated with the prototype with the Marx circuit with an output voltage of 4 kV. The output voltage of 4 kV is obtained.

References

[1] A. Zglav, Z. Kovacic and M. Balenovic, "Automatic Tuning Methodology for Automotive Lean NOx Trap Catalyst Using Response Data," 2018 6th International Symposium on Computational and Business Intelligence (ISCBI), pp. 41-47 (2018)

[2] P. Forzatti, L. Lietti, I. Nova, E. Tronconi, "Diesel NOx aftertreatment catalytic technologies: Analogies in LNT and SCR catalytic chemistry," Catalysis Today, Vol. 151, No. 3–4, pp. 202-211, Mar. 2010.

[3] Z. Salam, M. Facta and M. Amjad, "Dielectric Barrier Discharge Ozonizer Using the Transformerless Single-Switch Resonant Converter for Portable Applications," in IEEE Transactions on Industry Applications, vol. 50, no. 3, pp. 2197-2206 (2014)

[4] M. Okubo, N. Arita, T. Kuroki, "Total Diesel Emission Control Technology Using Ozone Injection and Plasma Desorption," Plasma Chemistry and Plasma Processing, Vol. 28, pp. 173-187, Apr. 2008.

[5] R. Cassel, "The evolution of pulsed modulators from the Marx generator to the Solid State Marx modulator and beyond," 2012 IEEE International Power Modulator and High Voltage Conference (IPMHVC) (2012)

[6] H. C. Bhosale, S. Bindu, G. Sincy, P. C. Saroj and S. Archana, "Design and simulation of 50 kv, 50 a solid state Marx generator," 2014 Annual International Conference on Emerging Research Areas: Magnetics, Machines and Drives (AICERA/iCMMD) (2014)

[7] T. Sakamoto and H. Akiyama, "Solid-State Dual Marx Generator With a Short Pulsewidth," IEEE Transactions on Plasma Science, Vol. 41, No. 10, pp. 2649-2653 (2013)

[8] K. TEHRANI, Y. LIU, L. ROUSSEAU, A. NORMAND and F. VURPILLOT, "Design of A Multistage Marx Generator topology based on SiC-MOSFET Device for Atomic Probe Tomography Applications," 2020 IEEE 15th International Conference of System of Systems Engineering (SoSE) (2020)

[9] L. M. Redondo, A. Kandratsyeu, M. J. Barnes and T. Fowler, "Design strategies for a SiC Marx generator for a kicker magnet," 2017 IEEE 21st International Conference on Pulsed Power (PPC) (2017)

[10] M. Hinojosa, H. O'Brien, E. Van Brunt, A. Ogunniyi and C. Scozzie, "Solid-state Marx generator with 24 KV 4H-SIC IGBTs," 2015 IEEE Pulsed Power Conference (PPC) (2015)

[11] J. Biela, M. Schweizer, S. Waffler and J. W. Kolar, "SiC versus Si—Evaluation of Potentials for Performance Improvement of Inverter and DC–DC Converter Systems by SiC Power Semiconductors," IEEE Transactions on Industrial Electronics, vol. 58, no. 7, pp. 2872-2882, July 2011

[12] K. Kusaka, Y. Ouchi and J. Itoh, "Gate Drive Power Supply for On-board Marx Circuit Using only Charging Path of Marx Capacitor," 2020 IEEE Energy Conversion Congress and Exposition (ECCE), 2020, pp. 3145-3150 (2020)

[13] D. Peftitsis, J. Rabkowski and H. Nee, "Self-Powered Gate Driver for Normally ON Silicon Carbide Junction Field-Effect Transistors Without External Power Supply," in IEEE Transactions on Power Electronics, vol. 28, no. 3, pp. 1488-1501 (2013)

[14] J. Itoh and T. Kinomae, "Experimental verification of a one-turn transformer power supply circuit for gate drive unit," Proceedings of 14th International Power Electronics and Motion Control Conference EPE-PEMC 2010 (2010)

[15] J. T. Strydom, M. A. de Rooij and J. D. van Wyk, "A comparison of fundamental gate-driver topologies for high frequency applications," Nineteenth Annual IEEE Applied Power Electronics Conference and Exposition, Vol. 2, pp. 1045-1052 (2004)

[16] J. Garcia, E. Gurpinar and A. Castellazzi, "High-frequency modulated secondary-side self-powered isolated gate driver for full range PWM operation of SiC power MOSFETs," 2017 IEEE Applied Power Electronics Conference and Exposition (APEC) (2017)

[17] Z. Ye, Y. Lei, W. Liu, P. S. Shenoy and R. C. N. Pilawa-Podgurski, "Improved Bootstrap Methods for Powering Floating Gate Drivers of Flying Capacitor Multilevel Converters and Hybrid Switched-Capacitor Converters," IEEE Transactions on Power Electronics, Vol. 35, No. 6, pp. 5965-5977 (2020)